



## Article

# Performance Evaluation of a Wet Medium Made of Mangosteen Peels for a Direct Evaporative Cooling System

Nattawut Chaomuang <sup>\*</sup>, Thanut Nuangjamnong and Samak Rakmae

Department of Food Engineering, School of Engineering, King Mongkut's Institute of Technology Ladkrabang, 1 Soi Chalongkrung 1, Ladkrabang, Bangkok 10520, Thailand

\* Correspondence: nattawut.ch@kmitl.ac.th

**Abstract:** The present study aimed to investigate an alternative evaporative cooling pad material made from mangosteen peel (MP) waste. Mangosteen peels were used to fill a 150 mm thick mesh container with a packing density of 180 kg/m<sup>3</sup>. A wind tunnel was constructed and utilized to experimentally evaluate the cooling performance of this organic-waste-based pad under hot and humid conditions (31–34 °C and 55–70% RH). The performance parameters assessed included pressure drop, temperature drop, saturation effectiveness, cooling capacity, and coefficient of performance (COP). The influence of air velocity (0.7, 1.0, 1.4, and 1.8 m/s) on these parameters was also examined. The results revealed that the saturation effectiveness of the MP pad ranged from 53% to 77% within the considered air velocity range. The maximum temperature drop (4.6 °C), saturation effectiveness (77%), cooling capacity (0.6 kW), and COP (3.5) were achieved when the system operated at 1.4 m/s. A comparative study showed that, at this velocity, the MP pad provided performance nearly equivalent to that of the commercial cellulose paper pad, except for the pressure drop. This result affirms the potential of mangosteen peels as a suitable wet medium for evaporative cooling applications.

**Keywords:** refrigeration; cooling pad; saturation effectiveness; valorization; vegetal waste



**Citation:** Chaomuang, N.; Nuangjamnong, T.; Rakmae, S. Performance Evaluation of a Wet Medium Made of Mangosteen Peels for a Direct Evaporative Cooling System. *AgriEngineering* 2023, 5, 1865–1878. <https://doi.org/10.3390/agriengineering5040114>

Academic Editors: Muhammad Sultan, Yuguang Zhou, Redmond R. Shamshiri and Muhammad Imran

Received: 2 September 2023  
Revised: 29 September 2023  
Accepted: 10 October 2023  
Published: 12 October 2023



**Copyright:** © 2023 by the authors. Licensee MDPI, Basel, Switzerland. This article is an open access article distributed under the terms and conditions of the Creative Commons Attribution (CC BY) license (<https://creativecommons.org/licenses/by/4.0/>).

## 1. Introduction

Among cooling technologies, vapor-compression refrigeration (VCR) is the dominant cooling system for cold storage [1]. Despite its high efficiency, this system is energy-intensive and greatly responsible for greenhouse gas emissions. Evaporative cooling systems have been deemed a viable alternative to VCR due to their simple structure, ease of maintenance, low capital and operating costs, and low environmental impacts [2]. They have been broadly implemented in various space cooling applications, such as in buildings [3,4], livestock barns [5], agricultural greenhouses [6], and horticultural product storage [7]. Numerous studies have extensively demonstrated the potential of evaporative cooling systems for the quality preservation of fruits and vegetables—for example, leafy vegetables [8], mangoes [9], peppers [10], and tomatoes [11,12]. Evaporative cooling is generally classified into two types: direct and indirect [13]. In a direct evaporative cooler, air is in direct contact with water, which can be either sprayed directly in air streams or supplied to a wet medium residing in the flow passage. The air is cooled down and humidified through water evaporation and subsequently supplied to a target space. On the other hand, indirect evaporative cooling involves two air streams. The first air stream is directly cooled and humidified through water evaporation and then used to cool the second air stream without humidification by a heat exchanger. The second air stream is then supplied to the target space. The applications of direct and indirect evaporative cooling systems rely on the humidification requirements [14]. For instance, direct evaporating cooling is preferable for cold storage of fruits and vegetables because of their high humidity requirement.

The wet medium, commonly called an “evaporative cooling pad” or simply “cooling pad”, is the key determinant for the performance of both direct and indirect evaporative

cooling systems. The systems incorporated with the cooling pads can apparently achieve superior cooling performance compared to those with direct water spraying [15]. Numerous studies have proposed various types of cooling pads to improve the performance of direct evaporative cooling [16]. Based on their material and configuration, the cooling pads can be categorized into fiber pads, rigid media pads, and packages or fill pads [17]. Rigid media pads made of corrugated cellulose paper are mostly used because of their large water-to-air contact areas, resulting in high saturation effectiveness and long lifespans. Franco-Salas and Peña-Fernández [18] experimentally compared the evaporative cooling performance of a brand-new rigid media pad with that of a 3-year-old used pad (same model). The results showed that the old pad achieved higher saturation effectiveness compared to the new one. The authors explained that the enhanced saturation effectiveness resulted from the salt incrustation on the pad, which caused an increase in the air–water contact time. Nada and Fouda [19] proposed a rigid media pad with a beehive structure. Its cooling performance was experimentally examined under various operating conditions (air velocity, inlet air temperature, water flow rate, water temperature, and pad thickness). It was found that the saturation effectiveness can be enhanced by increasing the pad thickness and water flow rate. However, the pad thickness should be selected with caution, because excessively thick cooling pads are often associated with high capital (i.e., price of cooling pads) and operating (i.e., energy consumption of fans) costs. Yan and He [20] experimentally investigated the influence of the cooling pad arrangements on the evaporative cooling performance. The results showed that a pair of cooling pads with a space in between them exhibited superior cooling effectiveness when compared with the case without spacing. This result suggests the possibility of using cooling pads of the same thickness to obtain the desired cooling effectiveness by leaving space between the pads.

The production of rigid media pads is complex and requires advanced machinery. Various materials have been proposed as alternatives for cooling pads, often in the form of fiber and fill pads. Table 1 presents fiber and fill pads made of different alternative materials based on natural and organic materials. Plastic-, metal-, and stone-based materials have also been investigated by numerous studies, which have been comprehensively reviewed in several papers [16,17,21].

**Table 1.** Experimental studies on fiber and fill pads made from natural and organic materials for direct evaporative cooling systems.

| Material             | Dimensions <sup>1</sup> | Air Velocity/<br>Flow Rate | Saturation<br>Effectiveness | Cooling<br>Capacity | Country      | Ref. |
|----------------------|-------------------------|----------------------------|-----------------------------|---------------------|--------------|------|
| Aspen<br>fibers      | 17 × 17 × 60            | 1.4 m/s                    | 71.6%                       | -                   | India        | [22] |
|                      | 40 × 40 × 7.5           | 5.44 m <sup>3</sup> /min   | 67–75%                      | -                   | Iran         | [23] |
|                      | 87 × 61 × 2.5           | 1.4 m/s                    | 52–67%                      | 0.5–1.6 kW          | India        | [24] |
|                      | 31 × 30 × 5             | 2.4 m/s                    | 49.5%                       | -                   | Saudi Arabia | [25] |
| Bulrush              | N.P.                    | 0.1–1.2 m/s                | 19–35%                      | 0.06–0.42 kW        | Turkey       | [21] |
| Coconut<br>fibers    | 30 × 30 × 15            | 0.5–4.0 m/s                | 83.5–93.8                   | 0.06–0.53 W         | China        | [26] |
|                      | 10 × 13.5 × 7           | 1.9–2.8 m/s                | 44.1–51.5%                  | -                   | Thailand     | [27] |
|                      | 17 × 17 × 60            | 1.4 m/s                    | 69.4%                       | -                   | India        | [22] |
|                      | 92 × 66 × 10            | 3.6–5.6 m/s                | 85%                         | -                   | Bangladesh   | [28] |
|                      | 10 × 10 × 10            | 0.062–0.083 kg/s           | 35–70%                      | 0.1–0.5 kW          | India        | [29] |
| Eucalyptus<br>fibers | 24 * × 10               | 0.03–0.08 kg/s             | 78%                         | 0.81                | Turkey       | [30] |
|                      | N.P.                    | 0.1–1.2 m/s                | 23–76%                      | 0.12–0.68 kW        | Turkey       | [21] |
| Jute fibers          | 31 × 30 × 5             | 2.4 m/s                    | 62.1%                       | -                   | Saudi Arabia | [25] |
|                      | 30 × 40 × 6             | 3.0–4.5 m/s                | 17.4–93.8                   | -                   | Nigeria      | [31] |
| Khus fibers          | 17 × 17 × 60            | 1.4 m/s                    | 64.2%                       | -                   | India        | [22] |
| Luffa fibers         | 31 × 30 × 5             | 2.4 m/s                    | 55.1%                       | -                   | Saudi Arabia | [25] |
|                      | 96 × 96 × 12.5          | 0.77 m/s                   | 57.0%                       | -                   | Brazil       | [32] |

Table 1. Cont.

| Material       | Dimensions <sup>1</sup> | Air Velocity/<br>Flow Rate | Saturation<br>Effectiveness | Cooling<br>Capacity | Country      | Ref. |
|----------------|-------------------------|----------------------------|-----------------------------|---------------------|--------------|------|
| Palash fibers  | 17 × 17 × 60            | 1.4 m/s                    | 81.0%                       | -                   | India        | [22] |
| Palm fibers    | 31 × 30 × 5             | 2.4 m/s                    | 38.9%                       | -                   | Saudi Arabia | [25] |
|                | 30 × 40 × 6             | 3.0–4.5 m/s                | 49.0–98.8%                  | -                   | Nigeria      | [31] |
| Rice husk      | 53 × 53 × 5.1           | 1–3 m/s                    | 55.4–61.9%                  | -                   | Thailand     | [33] |
| Sackcloth      | 92 × 66 × 10            | 3.6–5.6 m/s                | 69%                         | -                   | Bangladesh   | [28] |
| Straw fiber    | 600 × 200 × 10          | N.P.                       | 76%                         | -                   | Sudan        | [34] |
| Water hyacinth | 20 × 50 × 5             | 1.5–3.6 m/s                | 20–40%                      | -                   | Thailand     | [35] |
| Wood Chips     | 24 * × 10               | 0.03–0.08 kg/s             | 81%                         | 0.90 kW             | Turkey       | [30] |
|                | 10 × 10 × 10            | 0.062–0.083 kg/s           | 50–80%                      | 0.2–0.5 kW          | India        | [29] |
|                | 600 × 200 × 10          | N.P.                       | 90%                         | -                   | Sudan        | [34] |

<sup>1</sup> Width (cm) × height (cm) × thickness (cm); \* diameter (mm) of cylindrical pads. N.P. = data not provided.

As shown in Table 1, materials derived from organic waste exhibit potential as cooling pad materials since they can achieve saturation effectiveness comparable to commercial cellulose pads. The present study represents another attempt to explore the cooling performance of an organic cooling pad made from mangosteen peel waste. Mangosteen (*Garcinia mangostana* L.) is renowned as one of the world's most exquisite fruits, often referred to as the "Queen of Fruits" due to its sweet–sour taste and unique appearance, with sepals arranged like a crown [36]. Mangosteen is a tropical tree species primarily cultivated in Southeast Asian countries, such as Indonesia, Malaysia, and Thailand [37]. In 2020, Thailand alone produced nearly 340,000 tons of mangosteen, with approximately 290,000 tons of fresh mangosteen intended for export, leaving about 50,000 tons for domestic consumption [38]. It was estimated that 1 kg of mangosteen fruits can yield 0.6 kg of mangosteen peels [39]. According to this estimate, at least 30,000 tons of mangosteen peels were generated and treated as waste. The valorization of mangosteen peels would be a favorable approach to waste management. For instance, Nasrullah, Saad [39] employed mangosteen peel waste as a precursor for activated carbon, demonstrating its potential through batch adsorption studies for the removal of methylene from aqueous solutions. In the present study, mangosteen peel waste was harnessed as a cooling pad material due to its high porosity and water retention capacity. The high porosity of this organic cooling pad, derived from mangosteen peels, distinguishes it from other organic cooling pads discussed in the existing literature. Its performance was experimentally characterized in terms of temperature drop, saturation effectiveness, cooling capacity, coefficient of performance (*COP*), and pressure drop. The influence of air velocity on these performance parameters was also investigated, and the optimal air velocity was determined. Finally, the performance of the mangosteen peel waste-based cooling pad was compared with that of a commercial corrugated cellulose pad.

## 2. Materials and Methods

### 2.1. Experimental Setup

In this study, mangosteen peels (MPs) were proposed and utilized as an alternative cooling pad material for a direct evaporative cooling system. Initially, the mangosteen peels were sun-dried under uniform weather conditions for several days until their water activity ( $a_w$ ) reached a level below 0.6. The  $a_w$  was measured using a water activity analyzer (Aqualab 4TE, Meter group Inc., Pullman, WA, USA). Approximately 2.2 kg of the dried mangosteen peels were filled in a container (300 mm × 260 mm × 150 mm) constructed with aluminum wire mesh, resulting in a packing density of about 180 kg/m<sup>3</sup> (Figure 1a).

For comparative purposes, a commercial cooling pad made of corrugated cellulose papers (CPs) with identical dimensions (300 mm × 260 mm × 150 mm) was also employed and tested in the study (Figure 1b).

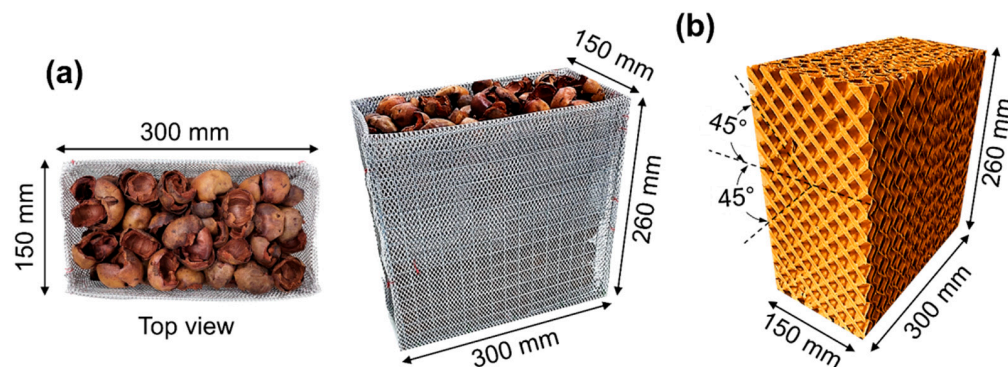


**Figure 1.** The cooling pads made from (a) mangosteen peels and (b) corrugated cellulose papers.

A wind tunnel with internal dimensions of 300 mm (width) × 260 mm (height) × 1500 mm (length) was constructed and used to investigate the cooling pad performance. The wind tunnel walls comprised two layers: an outer layer made of 8 mm thick acrylic plates and an inner insulation layer composed of 25 mm thick polyurethane foam boards. The insulation layer served to minimize heat losses from the system.

The test section was designed to accommodate a 150 mm thick cooling pad. This section featured a top-mounted water distribution system to evenly distribute water into the cooling pad, along with a bottom-mounted water collection system for draining excess water back into a 40 L water tank. A 40 W submersible pump (PRO-DS5000, Marine Plus Co., Ltd., Bangkok, Thailand) was employed to recirculate water from the tank to the water distribution system, maintaining a constant water flow rate of 250 L/h.

At the entrance of the wind tunnel, a 750 W centrifugal fan (SC-1304, Venz Industrial Co., Ltd., Bangkok, Thailand) was installed. The rotational speed of the fan motor was controlled using a variable frequency drive (MS300, Delta Electronics, Inc., Taiwan) to generate various air flow rates within the system. Based on a preliminary study, air velocities of 0.7, 1.0, 1.4, and 1.8 m/s were achieved by adjusting the input power frequencies to 20, 30, 40, and 50 Hz, respectively. It is important to note that these air velocities represent averages of 16 measurement points over the cross-sectional area of the wind tunnel using a hot-wire anemometer (405i, Testo SE & Co. KGaA, Titisee-Neustadt, Germany).

A depiction of the experimental arrangement can be found in Figure 2.

## 2.2. Experimental Procedure

Initially, the pressure drop across the cooling pad was measured for various flow rates using a digital manometer (510i, Testo SE & Co. KGaA, Germany). For each flow rate, data were recorded every 10 s for 30 min, and the average values were calculated for subsequent analysis. Subsequently, a series of experiments was conducted to evaluate the cooling pad performance. All experiments were conducted between 10:30 a.m. and 04:30 p.m. under real climate conditions in the months of June and August 2022 at our laboratory in Bangkok, Thailand (13.7269° N, 100.7722° E).

Before commencing each measurement, water circulation in the test section ran continuously for at least 30 min to ensure the saturation of the pad. In each experiment, the temperature and relative humidity of the air were measured before and after passing through the cooling pad every 30 s, using two temperature–humidity probes (probe diameter = 4 mm) connected to a data logger (176H1, Testo SE & Co. KGaA, Germany). Additionally, the temperature and relative humidity of the ambient air at two locations surrounding the wind tunnel were monitored every 1 minute using temperature–humidity data loggers (174H1, Testo SE & Co. KGaA, Germany). The specifications of the instruments

used in the experiments are given in Table 2. Each experiment was replicated three times to ensure the repeatability and reliability of the results.

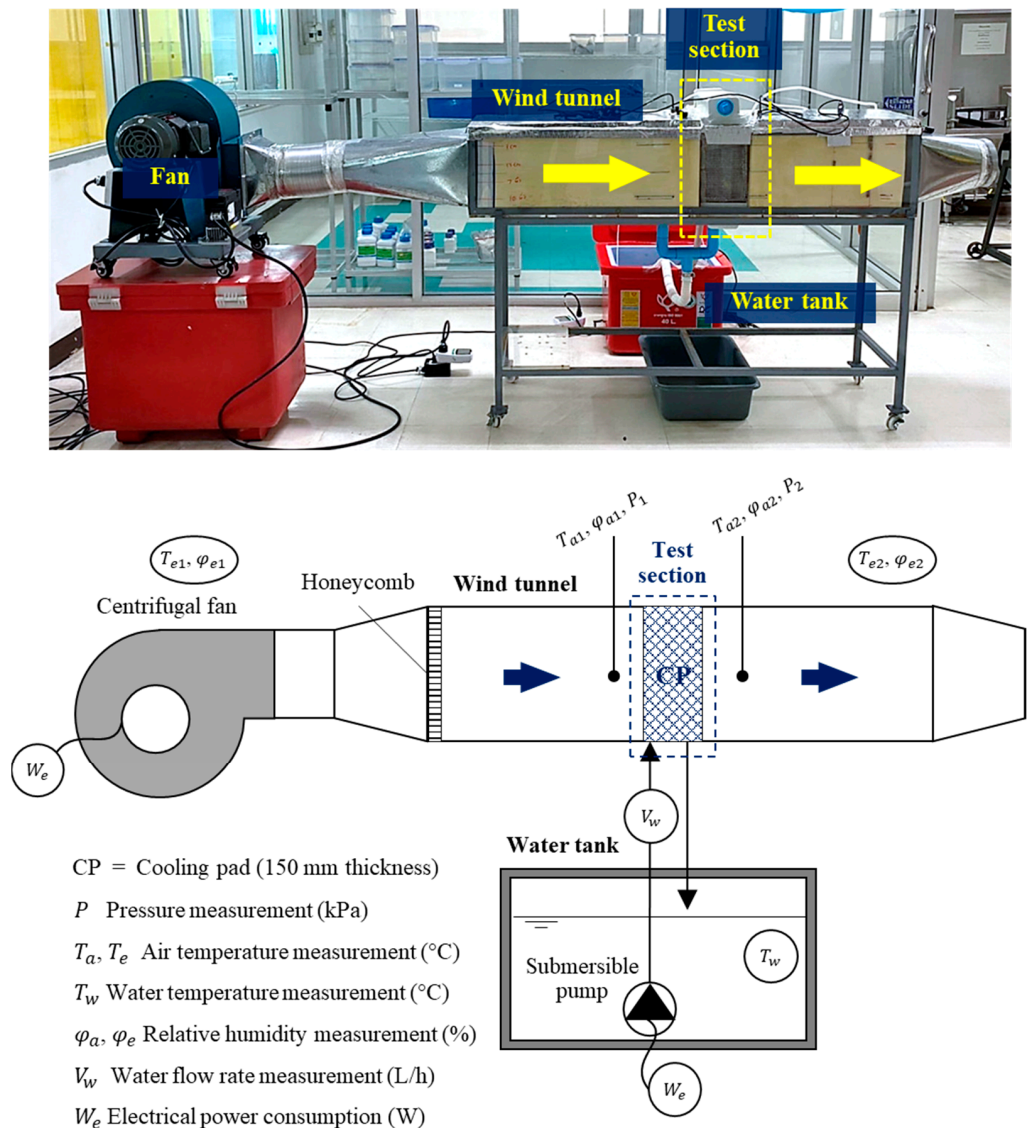


**Figure 2.** A schematic and photograph of experimental setup. Arrows indicate airflow direction across the test section.

**Table 2.** Specifications of the instruments.

| Parameter                         | Instrument                       | Accuracy                                       | Measuring Range  |
|-----------------------------------|----------------------------------|--|--|
| Air velocity                      | Hot-wire anemometer (Testo 405i) | $\pm 0.1$ m/s<br>$\pm 0.3$ m/s                 | 0 to 2 m/s<br>2 to 15 m/s                                      |
| Differential pressure             | Manometer (Testo 510i)           | $\pm 0.02$ kPa                                 | -15 to +15 kPa   |
| Electrical power consumption      | Wattmeter (Intertek)             | $\pm 2\%$ of measured data                     | 0 to 3680 W  |
| Temperature and relative humidity | Thermo-hygrometer (Testo 176H1)  | $\pm 0.2$ $^{\circ}\text{C}$<br>$\pm 2.0\%$ RH | -20 $^{\circ}\text{C}$ to +70 $^{\circ}\text{C}$<br>20% to 95% |
|                                   | Thermo-hygrometer (Testo 174H)   | $\pm 0.5$ $^{\circ}\text{C}$<br>$\pm 3.0\%$ RH | -20 to +70 $^{\circ}\text{C}$<br>2 to 98%                      |

### 2.3. Performance Evaluation

The evaporative cooling performance of the cooling pad was evaluated based on temperature drop, saturation effectiveness, cooling capacity, COP, and pressure drop. The formulas used for evaluating each of these parameters are detailed in the following subsections, with the exception of the pressure drop across the pad, which was derived from the measurements as previously explained in Section 2.2.

#### 2.3.1. Temperature Drop

Temperature drop is defined as the difference in the dry-bulb temperatures of the air entering ( $T_{a1}$ ) and leaving ( $T_{a2}$ ) the cooling pad, and is expressed as

$$\Delta T = T_{a1} - T_{a2} \tag{1}$$

#### 2.3.2. Saturation Effectiveness

In the literature, various terms have been used to denote a specific cooling pad ability to lower air temperature compared to the maximum temperature reduction achievable in direct evaporative cooling systems. These terms include cooling effectiveness or efficiency [40,41], saturation effectiveness or efficiency [21,42], wet-bulb effectiveness or efficiency [30,43], and humidification efficiency [44]. In fact, these terms share the same definition. However, the term “effectiveness” is considered more precise than “efficiency” as evaporative cooling does not involve energy conversion [17]. Therefore, this study adopts the term “saturation effectiveness”, which is expressed as the ratio of the difference between the dry-bulb temperatures of the inlet and outlet air to the difference between the dry-bulb and wet-bulb temperatures of the inlet air:

$$\varepsilon_s = \frac{T_{a1} - T_{a2}}{T_{a1} - T_{wb1}} = \frac{\Delta T}{T_{a1} - T_{wb1}} \tag{2}$$

An empirical equation was used to calculate the instantaneous wet-bulb temperature ( $T_{wb1}$ ) associated with the dry-bulb temperature ( $T_a$ ) and relative humidity ( $\varphi_a$ ) of inlet air, expressed as follows [45]:

$$T_{wb} = T_a \tan^{-1} \left[ b_1 (\varphi_a + b_2)^{0.5} \right] + \tan^{-1} (T_a + \varphi_a) - \tan^{-1} (\varphi_a - b_3) + b_4 \varphi_a^{1.5} \tan^{-1} (b_5 \varphi_a) - b_6 \tag{3}$$

The values in the arctangent function are in radians and the values of the coefficients  $b_i$  ( $i = 1$  to  $6$ ) are given in Table 3.

**Table 3.** The values of the coefficients used in Equation (3).

| $i$ | $b_i$      |
|-----|------------|
| 1   | 0.151977   |
| 2   | 8.313659   |
| 3   | 1.676331   |
| 4   | 0.00391838 |
| 5   | 0.023101   |
| 6   | 4.686035   |

#### 2.3.3. Cooling Capacity

The cooling capacity of the system is calculated using Equation (4). This equation signifies the amount of sensible energy extracted from the air to lower the temperature.

$$Q_c = \dot{m}_a c_{pa} (T_{a1} - T_{a2}) = \dot{m}_a c_{pa} \Delta T \tag{4}$$

The air mass flow rate ( $\dot{m}_a$ ) is defined as

$$\dot{m}_a = \rho_a A_c \bar{u}_a \quad (5)$$

In our case, the cross-sectional area ( $A_c$ ) of the cooling pad was about 0.078 m<sup>2</sup>, and the average air velocity ( $\bar{u}_a$ ) was derived from measurements taken at 16 points across the cross-sectional area.

The density ( $\rho_a$ ) and specific heat ( $c_{pa}$ ) of moist air are calculated using the following equations [46]:

$$\rho_a = \frac{M_{da}P}{R_u(T_a + 273.15) \left(1 + \frac{M_{da}}{M_{wv}} \omega_a\right)} \quad (6)$$

$$c_{pa} = c_{pda} + \omega_a c_{pww} \quad (7)$$

The humidity ratio ( $\omega_a$ ) represents the ratio of the mass of water vapor to the mass of dry air. In this study, it is determined using an empirical equation expressed as a function of the dry-bulb temperature and relative humidity [47]:

$$\omega = \frac{0.622 \left[ \alpha \frac{\phi}{100} \exp\left(\frac{\beta T}{\gamma + T}\right) \right]}{10P - \left[ \alpha \frac{\phi}{100} \exp\left(\frac{\beta T}{\gamma + T}\right) \right]} \quad (8)$$

The constant parameters for Equations (6) to (8) are provided in Table 4.

**Table 4.** The constant parameters for Equations (6) to (8).

| Parameter | Value     | Unit        |
|-----------|-----------|-------------|
| $c_{pda}$ | 1.006     | kJ/(kg·°C)  |
| $c_{pww}$ | 1.84      | kJ/(kg·°C)  |
| $M_{da}$  | 28.966    | kg/kmol     |
| $M_{wv}$  | 18.015268 | kg/kmol     |
| $P$       | 101.325   | kPa         |
| $R_u$     | 8.314472  | kJ/(kmol·K) |
| $\alpha$  | 0.6112    | kPa         |
| $\beta$   | 17.62     | -           |
| $\gamma$  | 243.12    | °C          |

#### 2.3.4. Coefficient of Performance

The coefficient of performance (COP) is defined as the ratio of the achieved cooling capacity to the total electrical power supplied to operate the fan and the pump.

$$COP = \frac{Q_c}{W_{ef} + W_{ep}} \quad (9)$$

The power consumption of the pump ( $W_{ep}$ ) remained constant at 6.1 W, as measured by a watt meter, because the water flow rate was not adjusted during the study. In contrast, the power consumption of the fan ( $W_{ef}$ ) varied with measurements of 57 W, 95 W, 162 W, and 270 W, obtained using a watt meter when the frequency was set to 20 Hz, 30 Hz, 40 Hz, and 50 Hz, respectively.

#### 2.4. Uncertainty Analysis

The propagation of error was used to quantify the uncertainty resulting from physical measurements of independent parameters such as temperature, relative humidity, and velocity, as described in references [48,49]. Given that  $y$  is a dependent variable expressed

as a function of independent variables  $x_k$ , which are derived from measurements and/or calculations,

$$y = f(x_1, x_2 \dots x_n) \quad (10)$$

The absolute uncertainty of the dependent variable ( $\sigma_y$ ) is then estimated from

$$\sigma_y = \sqrt{\left(\frac{dy}{dx_1}\sigma_{x_1}\right)^2 + \left(\frac{dy}{dx_2}\sigma_{x_2}\right)^2 + \dots + \left(\frac{dy}{dx_n}\sigma_{x_n}\right)^2} \quad (11)$$

The partial derivatives of the function with respect to the given independent variable ( $dy/dx_k$ ) were numerically computed using MATLAB software (MathWorks R2021b). The uncertainty of individual independent variables ( $\sigma_{x_k}$ ) obtained from measurements was based on the instrument accuracy (Table 2), while those obtained from calculations were determined by previously estimated uncertainties. The relative uncertainty ( $U_y$ ) was subsequently estimated using Equation (12).

$$U_y = \frac{\sigma_y}{|y|} \times 100 \quad (12)$$

Table 5 provides a summary of the maximum and minimum relative uncertainties for each performance parameter. Notably, all parameters exhibited uncertainties of less than 20%. While the maximum values may seem significant when expressed as percentages, it is important to note that they correspond to relatively small absolute variations.

**Table 5.** The relative uncertainty (%) of the performance parameters.

| Parameter       | Maximum | Minimum |
|-----------------|---------|---------|
| $\Delta T$      | 11.8    | 5.8     |
| $\varepsilon_s$ | 11.8    | 7.6     |
| $Q_c$           | 18.2    | 8.7     |
| $COP$           | 18.2    | 8.9     |

### 3. Results and Discussion

The cooling performance of the MP pad was evaluated by measuring the air temperature and relative humidity before and after the pad inside the wind tunnel. These measurements were conducted at four different air velocities (0.7, 1.0, 1.4, and 1.8 m/s), corresponding to mass flow rates of 0.06, 0.09, 0.12, and 0.15 kg/s, respectively. The water flow rate remained constant at 250 L/h for all experiments. The same experimental procedure was applied to the CP pad for the purpose of comparison. Each measurement was replicated three times, resulting in a total of twenty-four measurements. The collected data were used to determine the performance parameters, as explained in Section 2.3. The reported and analyzed values for each parameter represent the averages of the three replications.

#### 3.1. Verification of Steady State Condition

All experiments were conducted under real climate conditions. To minimize the variations in the results, data collected during a nearly steady state period of 3 h were extracted for each experiment and used for analysis. As shown in Figure 3, the average ambient air temperature and relative humidity during this period ranged from 30 °C to 34 °C and 55% to 70%, respectively. Moreover, within a given experiment, fluctuations in ambient air temperature ( $T_{a1,max} - T_{a1,min}$ ) never exceeded 2.0 °C, and relative humidity ( $\varphi_{a1,max} - \varphi_{a1,min}$ ) remained within 10%.

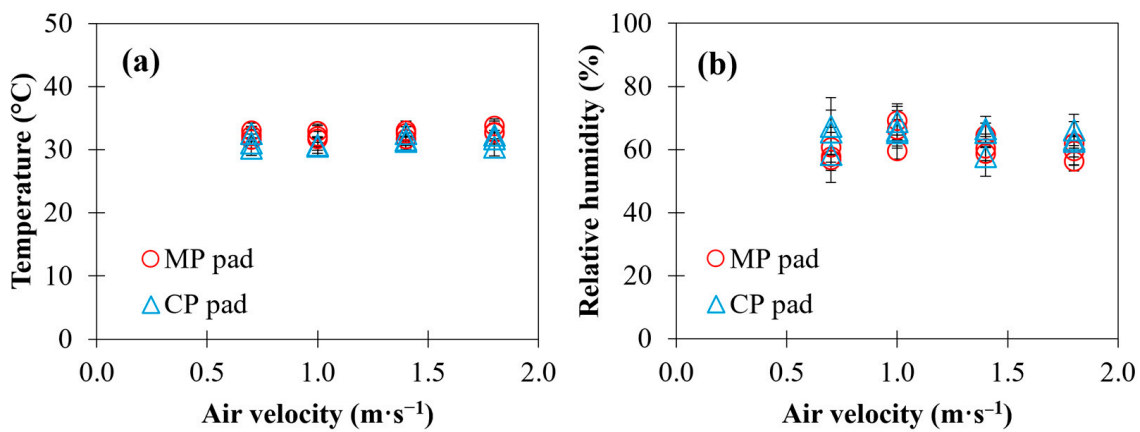


Figure 3. (a) Ambient air temperature and (b) relative humidity averaged over 3 h of the experiments.

### 3.2. Cooling Performance

A minimal pressure drop is considered an ideal characteristic for evaporative cooling pads [17]. As depicted in Figure 4, the pressure drop increased with higher air velocity, ranging from 14.7 Pa to 89.7 Pa. The standard deviations among replications were consistently less than 1.3 Pa. Pressure drops within this range are typical for organic-based cooling pads with similar thickness. For instance, a cooling pad made of fine fabric polyvinyl chloride (PVC) sponge mesh with a 150 mm thickness exhibited pressure drops of around 50–100 Pa at air velocities ranging from 1.5 m/s to 2.0 m/s [50]. In another study by Suranjan Salins, Reddy [29], increasing the flow rate from 0.062 kg/s to 0.083 kg/s resulted in pressure drops across the cooling pad that ranged from 47 Pa to 65 Pa for the coconut coir pad and from 50 Pa to 67 Pa for the wood shaving pad.

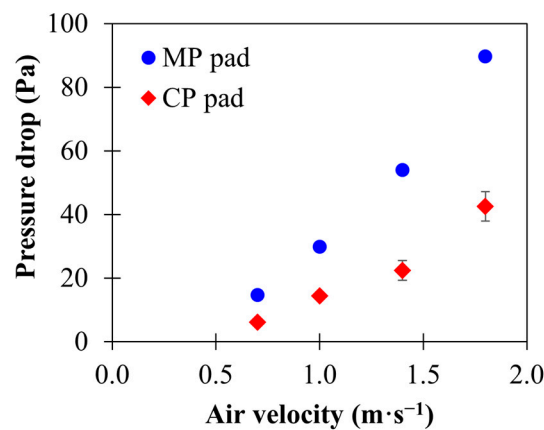


Figure 4. Pressure drops of the airflow across the cooling pads at different air velocities.

Figure 4 further illustrates that, at all considered air velocities, the MP pad produced a higher pressure drop than the CP pad (<50 Pa). This could be attributed to the relatively high packing density of the MP pad, resulting in a larger contact area and increased friction, consequently leading to greater pressure drops [29]. Ergun’s correlation is commonly used to describe the pressure drop through packed beds of particles, resulting from kinetic and viscous energy losses [51]. According to Ergun’s correlation, the viscous term is proportional to flow rate, while the kinetic (inertial) term is proportional to the flow rate squared. This explains the nonlinear increase in pressure drop across the MP pad with increased velocity, as shown in Figure 4.

As shown in Figure 5, the temperature drops achieved by the MP and CP pads were nearly identical, ranging between 3.4–4.6 °C for the MP pad and 3.5–4.4 °C for the CP pads.

These results align with previous findings in the literature, suggesting that air velocity has a relatively modest impact on air temperature reduction. For example, Rawangkul, Khedari [27] reported consistent temperature drops of 3.0 °C when using a coconut fiber cooling pad, even as air velocity increased from 1.9 m/s to 2.8 m/s. It is worth noting that the attainable temperature drop in evaporative cooling systems primarily hinges on the humidity level of the ambient air [52]. To achieve greater temperature drops, it is recommended to incorporate an air preconditioning unit, such as an air dehumidifier, into the system.

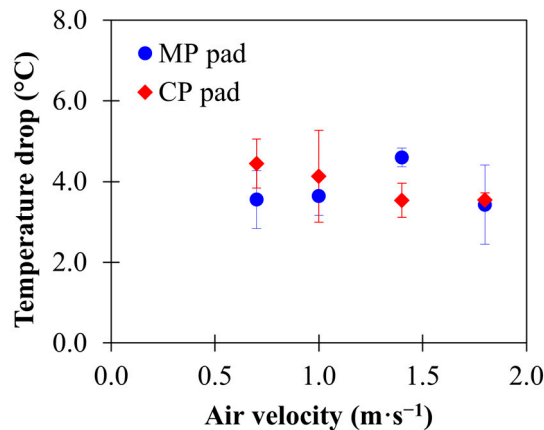


Figure 5. Variations of temperature drop across the MP and CP pads at different air velocities.

Saturation effectiveness demonstrates a direct relationship with temperature drop. As depicted in Figure 6, the saturation effectiveness of the MP pad experienced a slight increase, from 54% to 77%, as the air velocity increased from 0.7 to 1.4 m/s. However, at an air velocity of 1.8 m/s, the saturation effectiveness dropped to 53.0%. In contrast, the saturation effectiveness of the CP pad followed a declining trend with rising air velocity, decreasing from 81% at 0.7 m/s to 65% at 1.8 m/s. This decreasing trend aligns with common findings in the literature, where higher air velocity leads to shorter air-to-water interaction time, resulting in reduced saturation effectiveness [17]. It is important to note that the lower saturation effectiveness of the MP pad, compared to the CP pad at low air velocities (0.5–1.0 m/s), can be attributed to the observed pressure drop. Within this velocity range, the MP pad exhibited a higher pressure drop, resulting in shorter air-to-water interaction time compared to the CP pad.

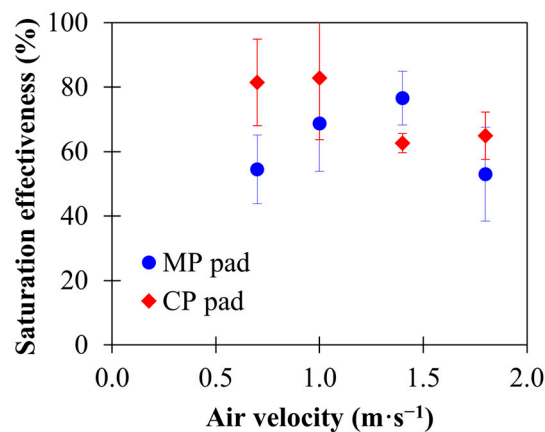
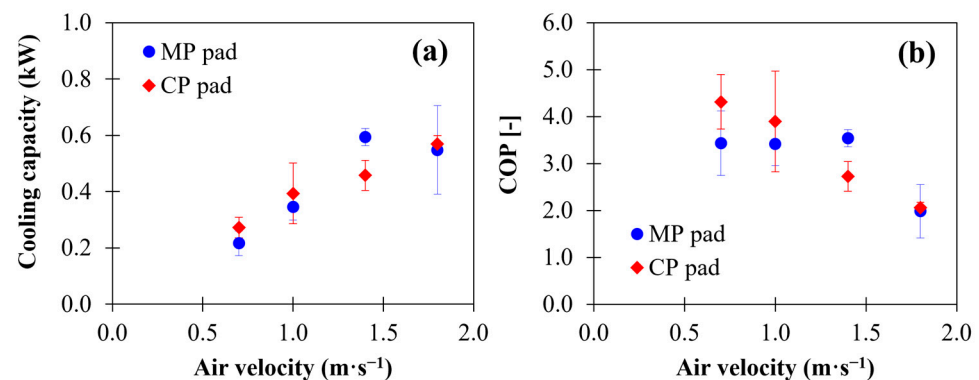


Figure 6. Saturation effectiveness of the MP and CP pads at different air velocities.

The observed contrary trend in the case of the MP pad at air velocities below 1.4 m/s is likely due to the enhanced heat and mass transfer coefficient between the air and the

packed bed of particles at higher velocities. These findings are consistent with those of Gunhan, Demir [53], who reported an increasing trend in saturation effectiveness with air velocity for coarse pumice stones. Despite the need for higher air velocity, the MP pad (77% at 1.4 m/s) demonstrated saturation effectiveness nearly on par with that of the CP pad (83% at 1.0 m/s) and other fiber and fill pads made of natural and organic materials, as summarized in Table 1.

Cooling capacity is another crucial performance parameter in evaporative cooling systems. It shows a direct relationship not only with temperature drop but also with flow rate. Despite the minor differences in temperature drops within the considered velocity range, cooling capacity increased with higher air velocity, as shown in Figure 7a. Notably, there was no significant difference between the cooling capacity of the MP pad (0.2–0.6 kW) and the CP pad (0.3–0.6 kW). Under the prevailing climate conditions, the MP pad achieved a maximum cooling capacity of nearly 0.60 kW when the system operated at 1.4 m/s.



**Figure 7.** (a) Cooling capacity and (b) coefficient of performance (*COP*) of the system with the MP and CP pads at different air velocities.

As illustrated in Figure 7b, the *COP* of the system with the MP pad remained around 3.5 within the air velocity range of 0.4–1.4 m/s. However, due to a substantial increase in fan power consumption, the *COP* dropped sharply to 2.0 at an air velocity of 1.8 m/s. In contrast, for the CP pad, the *COP* progressively decreased with increasing air velocity. Notably, the *COP* of the MP pad closely resembled that of other organic-based materials, such as eucalyptus fibers (*COP* = 3.8 at 0.04 kg/s) [21] and wood shaving (*COP* = 2.1 at 0.0083 kg/s) [29].

Overall, the MP pad exhibited comparable performance to the commercial CP pad in terms of temperature drop, saturation effectiveness, cooling capacity, and *COP*, except for the pressure drop. These findings underscore the potential of mangosteen peels as an alternative wet medium for evaporative cooling applications. However, the organic nature of the MP pad presents certain drawbacks. Like many natural materials, it is susceptible to bacteria and fungi growth when exposed to water for extended periods, necessitating regular cleaning and sterilization [21]. To mitigate microbial growth, the use of an air filter with pore sizes of less than 0.1  $\mu\text{m}$  is recommended to prevent the spread of bacteria and flora in the cooling space [54]. Moreover, prolonged use of the MP pad can lead to the production of unpleasant odors, particularly with mangosteen, which has a distinctive aroma. This drawback might limit the application of the MP pad in residential and building cooling, but it is less of an issue for storing horticultural products, such as mangosteen fruit itself.

#### 4. Conclusions

The present study investigated an alternative wet medium made from mangosteen peels for evaporative cooling systems. Its cooling performance was experimentally investigated and compared to that of a commercial corrugated cellulose paper pad. The results revealed that the optimum air velocity to operate the evaporative cooling system with the

MP pad was 1.4 m/s. At this velocity, the MP pad achieved a maximum temperature drop of 4.6 °C, a saturation effectiveness of 77%, a cooling capacity of 0.59 kW, and a COP of 3.5 while maintaining a tolerable pressure drop of 54 Pa. These findings demonstrate that its performance is on par with that of the commercial cellulose paper pad, opening the door to the potential valorization of mangosteen peel waste. Given its organic nature and distinctive aroma, the MP pad is best suited for horticultural product storage or applications tolerable of odors.

Evaporative cooling systems are typically not recommended for use in areas with hot and humid climates, such as in Thailand. For future works, it is advisable to explore hybrid systems that combine evaporative cooling with a water-cooling unit or desiccant dehumidifier to enhance the performance of this organic-waste-based cooling pad.

**Author Contributions:** Conceptualization, N.C. and S.R.; methodology, N.C. and S.R.; software, N.C.; validation, N.C., T.N. and S.R.; formal analysis, N.C., T.N. and S.R.; investigation, N.C. and T.N.; resources, N.C.; data curation, N.C., T.N. and S.R.; writing—original draft preparation, N.C.; writing—review and editing, N.C.; visualization, N.C.; supervision, N.C. and S.R.; project administration, N.C.; funding acquisition, N.C. All authors have read and agreed to the published version of the manuscript.

**Funding:** This work was financially supported by King Mongkut's Institute of Technology Ladkrabang, Thailand, grant number 2564-02-01-012.

**Data Availability Statement:** The data used in this study can be obtained upon request from the corresponding author.

**Acknowledgments:** The authors appreciate and acknowledge the support from Takahashi Foundation. Special thanks are given to Denis Flick (AgroParisTech, France) for his guidance and suggestions.

**Conflicts of Interest:** The authors declare no conflict of interest.

## References

1. Pezzutto, S.; Quaglini, G.; Riviere, P.; Kranzl, L.; Novelli, A.; Zambito, A.; Wilczynski, E. Screening of cooling technologies in Europe: Alternatives to vapour compression and possible market developments. *Sustainability* **2022**, *14*, 2971. [\[CrossRef\]](#)
2. Rafique, M.M.; Gandhidasan, P.; Rehman, S.; Al-Hadhrani, L.M. A review on desiccant based evaporative cooling systems. *Renew. Sustain. Energy Rev.* **2015**, *45*, 145–159. [\[CrossRef\]](#)
3. Fong, K.; Lee, C. Solar desiccant cooling system for hot and humid region—A new perspective and investigation. *Sol. Energy* **2020**, *195*, 677–684. [\[CrossRef\]](#)
4. Pandelidis, D.; Niemierka, E.; Pacak, A.; Jadwiszczak, P.; Cichoń, A.; Drag, P.; Worek, W.; Cetin, S. Performance study of a novel dew point evaporative cooler in the climate of central Europe using building simulation tools. *Build. Environ.* **2020**, *181*, 107101. [\[CrossRef\]](#)
5. Kashif, M.; Niaz, H.; Sultan, M.; Miyazaki, T.; Feng, Y.; Usman, M.; Shahzad, M.W.; Niaz, Y.; Waqas, M.M.; Ali, I. Study on desiccant and evaporative cooling systems for livestock thermal comfort: Theory and experiments. *Energies* **2020**, *13*, 2675. [\[CrossRef\]](#)
6. Ghoullem, M.; El Moueddeb, K.; Nehdi, E.; Boukhanouf, R.; Calautit, J.K. Greenhouse design and cooling technologies for sustainable food cultivation in hot climates: Review of current practice and future status. *Biosyst. Eng.* **2019**, *183*, 121–150. [\[CrossRef\]](#)
7. Nkolisa, N.; Magwaza, L.S.; Workneh, T.S.; Chimphango, A. Evaluating evaporative cooling system as an energy-free and cost-effective method for postharvest storage of tomatoes (*Solanum lycopersicum* L.) for smallholder farmers. *Sci. Hortic.* **2018**, *241*, 131–143. [\[CrossRef\]](#)
8. Ambuko, J.; Wanjiru, F.; Chemining'wa, G.; Owino, W.; Mwachoni, E. Preservation of postharvest quality of leafy amaranth (*Amaranthus* spp.) vegetables using evaporative cooling. *J. Food Qual.* **2017**, *2017*, 5303156. [\[CrossRef\]](#)
9. Kipruto, K.M. Effect of near infrared reflection and evaporative cooling on quality of mangoes. *Agric. Eng. Int. CIGR J.* **2017**, *19*, 162–168.
10. Samira, A.; Woldetsadik, K.; Workneh, T.S. Postharvest quality and shelf life of some hot pepper varieties. *J. Food Sci. Technol.* **2013**, *50*, 842–855. [\[CrossRef\]](#)
11. Babaremu, K.; Adekanye, T.; Okokpujie, I.; Fayomi, J.; Atiba, O. The significance of active evaporative cooling system in the shelf life enhancement of vegetables (red and green tomatoes) for minimizing post-harvest losses. *Procedia Manuf.* **2019**, *35*, 1256–1261. [\[CrossRef\]](#)
12. Sibanda, S.; Workneh, T.S. Effects of indirect air cooling combined with direct evaporative cooling on the quality of stored tomato fruit. *CyTA-J. Food* **2019**, *17*, 603–612. [\[CrossRef\]](#)

13. Yang, Y.; Cui, G.; Lan, C.Q. Developments in evaporative cooling and enhanced evaporative cooling—A review. *Renew. Sustain. Energy Rev.* **2019**, *113*, 109230. [[CrossRef](#)]
14. Xuan, Y.; Xiao, F.; Niu, X.; Huang, X.; Wang, S. Research and application of evaporative cooling in China: A review (I)—Research. *Renew. Sustain. Energy Rev.* **2012**, *16*, 3535–3546. [[CrossRef](#)]
15. Naveenprabhu, V.; Suresh, M. Performance enhancement studies on evaporative cooling using volumetric heat and mass transfer coefficients. *Numer. Heat Transf. Part A Appl.* **2020**, *78*, 504–523. [[CrossRef](#)]
16. Kumar, S.; Singh, J.; Siyag, J.; Rambhatla, S. Potential alternative materials used in evaporative coolers for sustainable energy applications: A review. *Int. J. Air-Cond. Refrig.* **2020**, *28*, 2030006. [[CrossRef](#)]
17. Tejero-González, A.; Franco-Salas, A. Optimal operation of evaporative cooling pads: A review. *Renew. Sustain. Energy Rev.* **2021**, *151*, 111632. [[CrossRef](#)]
18. Franco-Salas, A.; Peña-Fernández, A.; Valera-Martínez, D.L. Refrigeration capacity and effect of ageing on the operation of cellulose evaporative cooling pads, by wind tunnel analysis. *Int. J. Environ. Res. Public Health* **2019**, *16*, 4690. [[CrossRef](#)]
19. Nada, S.; Fouda, A.; Mahmoud, M.; Elattar, H. Experimental investigation of energy and exergy performance of a direct evaporative cooler using a new pad type. *Energy Build.* **2019**, *203*, 109449. [[CrossRef](#)]
20. Yan, M.; He, S.; Li, N.; Huang, X.; Gao, M.; Xu, M.; Miao, J.; Lu, Y.; Hooman, K.; Che, J. Experimental investigation on a novel arrangement of wet medium for evaporative cooling of air. *Int. J. Refrig.* **2021**, *124*, 64–74. [[CrossRef](#)]
21. Doğramacı, P.A.; Aydın, D. Comparative experimental investigation of novel organic materials for direct evaporative cooling applications in hot-dry climate. *J. Build. Eng.* **2020**, *30*, 101240. [[CrossRef](#)]
22. Jain, J.; Hindoliya, D. Correlations for saturation efficiency of evaporative cooling pads. *J. Inst. Eng. India Ser. C* **2014**, *95*, 5–10. [[CrossRef](#)]
23. Lotfizadeh, H.; Razzaghi, H.; Layeghi, M. Experimental performance analysis of a solar evaporative cooler with three different types of pads. *J. Renew. Sustain. Energy* **2013**, *5*, 063113. [[CrossRef](#)]
24. Bishoyi, D.; Sudhakar, K. Experimental performance of a direct evaporative cooler in composite climate of India. *Energy Build.* **2017**, *153*, 190–200. [[CrossRef](#)]
25. Al-Sulaiman, F. Evaluation of the performance of local fibers in evaporative cooling. *Energy Convers. Manag.* **2002**, *43*, 2267–2273. [[CrossRef](#)]
26. Liao, C.M.; Singh, S.; Wang, T.S. Characterizing the performance of alternative evaporative cooling pad media in thermal environmental control applications. *J. Environ. Sci. Health Part A* **1998**, *33*, 1391–1417. [[CrossRef](#)]
27. Rawangkul, R.; Khedari, J.; Hirunlabh, J.; Zeghmami, B. Performance analysis of a new sustainable evaporative cooling pad made from coconut coir. *Int. J. Sustain. Eng.* **2008**, *1*, 117–131. [[CrossRef](#)]
28. Alam, M.F.; Sazidy, A.S.; Kabir, A.; Mridha, G.; Litu, N.A.; Rahman, M.A. An experimental study on the design, performance and suitability of evaporative cooling system using different indigenous materials. In Proceedings of the 7th Bsme International Conference on Thermal Engineering, Dhaka, Bangladesh, 22–24 December 2016; p. 020075.
29. Suranjan Salins, S.; Reddy, S.K.; Kumar, S. Experimental investigation on use of alternative innovative materials for sustainable cooling applications. *Int. J. Sustain. Eng.* **2021**, *14*, 1207–1217. [[CrossRef](#)]
30. Khosravi, N.; Aydın, D.; Nejhad, M.K.; Dogramaci, P.A. Comparative performance analysis of direct and desiccant assisted evaporative cooling systems using novel candidate materials. *Energy Convers. Manag.* **2020**, *221*, 113167. [[CrossRef](#)]
31. Ndukwu, M.C.; Manuwa, S.I. Techno-economic assessment for viability of some waste as cooling pads in evaporative cooling system. *Int. J. Agric. Biol. Eng.* **2015**, *8*, 151–158. [[CrossRef](#)]
32. de Melo Júnior, J.C.F.; Bamberg, J.V.M.; Machado, N.S.; Caldas, E.N.G.; Rodrigues, M.S. Evaporative cooling efficiency of pads consisting of vegetable loofah. *Commun. Sci.* **2019**, *10*, 38–44. [[CrossRef](#)]
33. Soponpongpipat, N.; Kositchaimongkol, S. Recycled high-density polyethylene and rice husk as a wetted pad in evaporative cooling system. *Am. J. Appl. Sci.* **2011**, *8*, 186–191. [[CrossRef](#)]
34. Ahmed, E.M.; Abaas, O.; Ahmed, M.; Ismail, M.R. Performance evaluation of three different types of local evaporative cooling pads in greenhouses in Sudan. *Saudi J. Biol. Sci.* **2011**, *18*, 45–51. [[CrossRef](#)] [[PubMed](#)]
35. Ubonwat, J. A Feasibility Study of Using Water Hyacinth as Wetted Media in Evaporative Cooling System. Master's Thesis, King Mongkut's Institute of Technology Thonburi, Bangkok, Thailand, 2001.
36. Choodej, S.; Koopklang, K.; Raksat, A.; Chuaypen, N.; Pudhom, K. Bioactive xanthenes, benzophenones and biphenyls from mangosteen root with potential anti-migration against hepatocellular carcinoma cells. *Sci. Rep.* **2022**, *12*, 8605. [[CrossRef](#)] [[PubMed](#)]
37. Aizat, W.M.; Ahmad-Hashim, F.H.; Jaafar, S.N.S. Valorization of mangosteen, “The Queen of Fruits,” and new advances in postharvest and in food and engineering applications: A review. *J. Adv. Res.* **2019**, *20*, 61–70. [[CrossRef](#)]
38. Office of Agricultural Economics. *Agricultural Statistics of Thailand 2020*; Ministry of Agriculture & Cooperatives: Bangkok, Thailand, 2020.
39. Nasrullah, A.; Saad, B.; Bhat, A.; Khan, A.S.; Danish, M.; Isa, M.H.; Naem, A. Mangosteen peel waste as a sustainable precursor for high surface area mesoporous activated carbon: Characterization and application for methylene blue removal. *J. Clean. Prod.* **2019**, *211*, 1190–1200. [[CrossRef](#)]
40. Laknizi, A.; Ben Abdallah, A.; Faqir, M.; Essadiqi, E.; Dhimdi, S. Performance characterization of a direct evaporative cooling pad based on pottery material. *Int. J. Sustain. Eng.* **2021**, *14*, 46–56. [[CrossRef](#)]

41. Yan, M.; He, S.; Gao, M.; Xu, M.; Miao, J.; Huang, X.; Hooman, K. Comparative study on the cooling performance of evaporative cooling systems using seawater and freshwater. *Int. J. Refrig.* **2021**, *121*, 23–32. [[CrossRef](#)]
42. Velasco-Gómez, E.; Tejero-González, A.; Jorge-Rico, J.; Rey-Martínez, F.J. Experimental investigation of the potential of a new fabric-based evaporative cooling pad. *Sustainability* **2020**, *12*, 7070. [[CrossRef](#)]
43. Zhang, H.; Ma, H.; Ma, S. Investigation on indirect evaporative cooling system integrated with liquid dehumidification. *Energy Build.* **2021**, *249*, 111179. [[CrossRef](#)]
44. Kumar, S.; Salins, S.S.; Reddy, S.K.; Nair, P.S. Comparative performance analysis of a static & dynamic evaporative cooling pads for varied climatic conditions. *Energy* **2021**, *233*, 121136. [[CrossRef](#)]
45. Stull, R. Wet-bulb temperature from relative humidity and air temperature. *J. Appl. Meteorol. Climatol.* **2011**, *50*, 2267–2269. [[CrossRef](#)]
46. Gately, D.P. *Understanding Psychrometrics*, 3rd ed.; ASHRAE: Atlanta, GA, USA, 2013; p. 259.
47. Sensirion. *Introduction to Humidity: Basic Principles on Physics of Water Vapor*; Sensirion, The Sensor Company: Chicago, IL, USA, 2009.
48. Moffat, R.J. Describing the uncertainties in experimental results. *Exp. Therm. Fluid Sci.* **1988**, *1*, 3–17. [[CrossRef](#)]
49. Taylor, J. *Introduction to Error Analysis, the Study of Uncertainties in Physical Measurements*; University Science Books: Dulles, VA, USA, 1997.
50. Liao, C.-M.; Chiu, K.-H. Wind tunnel modeling the system performance of alternative evaporative cooling pads in Taiwan region. *Build. Environ.* **2002**, *37*, 177–187. [[CrossRef](#)]
51. Coker, A.K. 4—FLUID FLOW. In *Ludwig's Applied Process Design for Chemical and Petrochemical Plants*, 4th ed.; Coker, A.K., Ed.; Gulf Professional Publishing: Burlington, VT, USA, 2007; pp. 133–302. [[CrossRef](#)]
52. Laknizi, A.; Mahdaoui, M.; Abdellah, A.B.; Anoune, K.; Bakhouya, M.; Ezbakhe, H. Performance analysis and optimal parameters of a direct evaporative pad cooling system under the climate conditions of Morocco. *Case Stud. Therm. Eng.* **2019**, *13*, 100362. [[CrossRef](#)]
53. Gunhan, T.; Demir, V.; Yagcioglu, A. Evaluation of the suitability of some local materials as cooling pads. *Biosyst. Eng.* **2007**, *96*, 369–377. [[CrossRef](#)]
54. Chen, X.; Su, Y.; Aydin, D.; Ding, Y.; Zhang, S.; Reay, D.; Riffat, S. A novel evaporative cooling system with a polymer hollow fibre spindle. *Appl. Therm. Eng.* **2018**, *132*, 665–675. [[CrossRef](#)]

**Disclaimer/Publisher's Note:** The statements, opinions and data contained in all publications are solely those of the individual author(s) and contributor(s) and not of MDPI and/or the editor(s). MDPI and/or the editor(s) disclaim responsibility for any injury to people or property resulting from any ideas, methods, instructions or products referred to in the content.